Bis(1,2,6,7-tetracyano-3,5-dihydro-3,5-diiminopyrrolizinido) Complexes of Iron and Cobalt: Properties, Crystal Structures and Interaction with Dioxygen†

Mario Bonamico, Vincenzo Fares,* Alberto Flamini* and Nicola Poli
Istituto di Teoria e Struttura Elettronica dei Composti di Coordinazione del C.N.R., Area della Ricerca di Roma, P.O. Box 10, 00016 Monterotondo Stazione, Roma, Italy

The synthesis and characterization of complexes of the ligand 1,2,6,7-tetracyano-3,5-dihydro-3,5-diiminopyrrolizinide, $[ML_2]\cdot nA$ (M = Fe **1** or Co **2**; A = crystallization solvent) are described. For A = 1,2-dimethoxyethane (dme), $n = 2$, the compounds are isomorphous and isostructural as shown by crystal structure determinations. The central metal atom, which lies on a symmetry centre, co-ordinates four imino groups in a square-planar arrangement within the ligand equatorial plane, and completes its octahedral, tetragonally distorted $MN^{eq}_4N^{ax}_2$ co-ordination geometry with two axial cyano groups from two crystallographically equivalent complex molecules. The only significant difference between the two structures is confined to the M–N bond distances [Fe–N_{eq} 2.090(5); Fe–N_{ax} 2.295(5); Co–N_{eq} 2.017(5); Co–N_{ax} 2.369(5) Å]. Variable-temperature magnetic measurements on these two complexes reveal that they are both high-spin species ($S = 2$ and $\frac{3}{2}$, respectively) with antiferromagnetic superexchange interactions, which are stronger when M = Co. The optical spectra of both sets of complexes are very similar to those of corresponding metal phthalocyanines. Also, both can be chemically oxidized by using O_2 as oxidant in MeCN solution to give insoluble polymeric species, corresponding analytically to the formulae $[FeL_3(O_2)]\cdot 6MeCN$ and $[CoL_2(O_2)]\cdot 4MeCN$. These complexes are shown to be superoxo adducts in which the dioxygen is centrosymmetrically bridged between the metal atoms in the formal oxidation state Fe^{IV} and Co^{III} respectively.

In a recent paper[1] regarding the novel class of complexes bis(1,2,6,7-tetracyano-3,5-dihydro-3,5-diiminopyrrolizinido)-metal(II) $[ML_2]$ we have emphasized their peculiar features, as planar, centrosymmetric, electron-acceptor molecules, exhibiting a metal phthalocyanine-like optical spectrum. Given the continuing, considerable, wide-ranging interest in metal phthalocyanines[2] as photoconductors, semiconductors, functional dyes, oxidation catalysts and models for haem proteins, we are carrying out extensive research on the complexes $[ML_2]$ by varying the metal in order to establish the occurrence, stability and properties throughout the Periodic Table, in view of their analogy with the phthalocyanines.

Earlier we reported on copper(II)[3] and nickel(II)[1] derivatives; this paper describes the preparation and properties of iron(II) and cobalt(II) analogues and the crystal structures of their adducts with dimethoxyethane (dme): $[FeL_2]\cdot 2dme$ **1a** and $[CoL_2]\cdot 2dme$ **2a**. The reactivity with dioxygen is also examined.

Results and Discussion

Characterization of Complexes **1** *and* **2**.—*Crystal structures of* **1a** *and* **2a**. The crystal structures resemble that found in $[CuL_2]\cdot 2thf$ (thf = tetrahydrofuran):[3] the central metal atom, which lies on a symmetry centre, co-ordinates four imino groups from two diiminopyrrolizinido units, in a square-planar arrangement within the ligands equatorial plane, and completes its octahedral, tetragonally distorted $M^{II}N_4N'_2$ co-ordination geometry with two axial cyano groups from two crystallographically equivalent complex molecules (Fig. 1). The result is a three-dimensional network of almost orthogonal complex units.

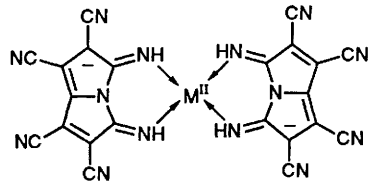

$[ML_2]$

M = Fe **1** or Co **2**
Molecules of crystallization : 2 dme **a**, 4 thf **b**, *n* MeCN **c** or *n* Me_2CO **d**

Two laterally adducted dme solvent molecules, similarly to the thf molecules in the copper derivative, are situated such that one of the two oxygen atoms, at a distance of 0.85 Å from the equatorial plane, weakly interacts with the ligands imino groups, at 2.912(8) and 2.992(9) Å from N(8) and N(14′) respectively (Fig. 2). In Table 4 bond distances and angles for both complexes **1a** and **2a** are shown. The ligand backbone has the same charge distribution and related geometry as found in $[CuL_2]\cdot 2thf$,[3] $[NiL_2]\cdot ttf\cdot 2thf$ (ttf = tetrathiafulvalene) and $[NiL_2]\cdot 3dioxane\cdot 2H_2O$,[1] which were only slightly influenced, in their inner part nearer the co-ordination centre, by the metal electronic configuration. In this case, however, no significant difference between d^6 Fe^{II} in **1a** and d^7 Co^{II} in **2a** can be noted.

A higher degree of tetragonal distortion is evident for the cobalt derivative, the Co–N(18′) axial bond being much more elongated [Co–N_{ax} 2.369(5) *vs.* Co–N_{eq} 2.017(5); Fe–N_{ax} 2.295(5) *vs.* Fe–N_{eq} 2.090(5) Å].

The Fe–N_{eq} distance value of 2.09 Å is larger than those observed in low-spin analogous iron(II) aza complexes like those of diiminosuccinonitrile[4a] or benzoquinone diimine[4b] (1.87–2.00 Å) and also in low-spin[4c–f] and in intermediate-

† *Supplementary data available:* see Instructions for Authors, *J. Chem. Soc., Dalton Trans.*, 1992, Issue 1, pp. xx–xxv.

Non-SI unit employed: eV ≈ 1.60 × 10^{-19} J.

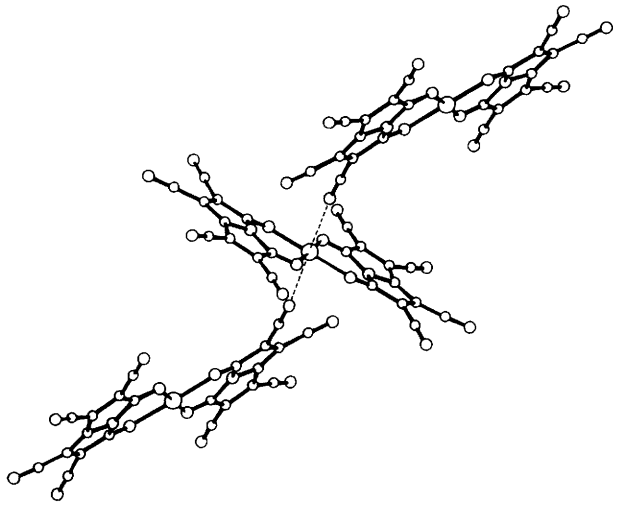

Fig. 1 Partial view of the crystal packing of complexes **1a** and **2a**, showing the axial interactions (broken lines) between the central metal atom and peripheral cyano-groups from crystallographically equivalent molecules

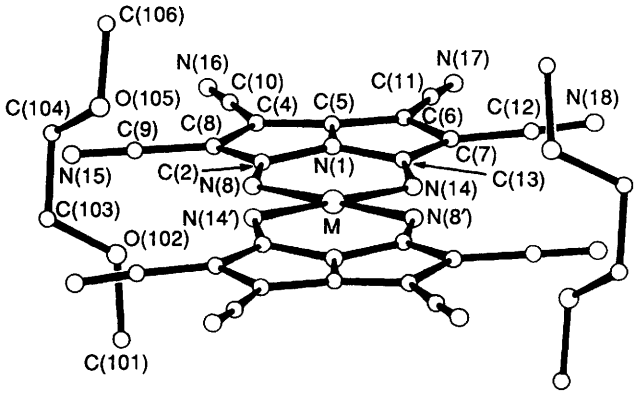

Fig. 2 Labelling scheme and perspective drawing of $[ML_2]\cdot 2dme$, showing the dme chains developing in a direction orthogonal to the complex plane

Table 1 Crystal data and experimental details for compounds **1a** and **2a**

Compound	**2a** $[FeL_2]\cdot 2dme$	**3a** $[CoL_2]\cdot 2dme$
Formula	$C_{30}H_{24}FeN_{14}O_4$	$C_{30}H_{24}CoN_{14}O_4$
M	700.463	703.549
a/Å	12.177(9)	12.123(5)
b/Å	11.053(8)	11.129(5)
c/Å	12.085(5)	12.826(5)
β/°	109.61(5)	110.57(4)
U/Å^3	1623(2)	1620(1)
D_c/g cm^{-3}	1.433	1.433
$F(000)$	720	722
Crystal dimensions/mm	0.8 × 0.3 × 0.15	0.4 × 0.4 × 0.4
μ/cm^{-1}	5.419	6.157
Transmission coefficients	0.75–0.95	0.80–0.85
No. of unique data	3702	3519
No. with $I \geqslant 3\sigma(I)$	1683	1852
Refined parameters	223	223
Data per parameters	7.5	8.3
R	0.0655	0.0622
R'	0.0632	0.0632

* Details in common: monoclinic, space group $P2_1/a$; deep blue prisms (under transmitted light); 25 °C; $Z = 2$; 2θ range 3–55°.

spin ($S = 1$)[5] rigid-core phthalocyanines or tetraphenylporphyrins (1.91–2.00 Å), while it is comparable with the values (2.08–2.12 Å) found in the few high-spin iron(II) aza complexes reported[6] (although the spin state $S = 2$ is here associated with five-co-ordination). Such an effect is usually related to the out-of-plane displacement of the metal atom from the equatorial plane due to the antibonding character of the $d_{x^2-y^2}$ orbital, which is semi-occupied in such high-spin complexes. On this basis, six-co-ordination should occur if accompanied by a change to a low-spin configuration, where $d_{x^2-y^2}$ is empty. Since the magnetic moment of complex **1a** is clearly consistent with four unpaired electrons (see below), it represents an example of a six-co-ordinated iron aza complex in a high-spin configuration, which must be related to the particularly low ligand-field strength. Also in the case of the cobalt complex **2a**, the observed $Co-N_{eq}$ distance of 2.02 is longer than the values (1.82 Å) found in the analogous low-spin cobalt(II) benzoquinonediimine,[4b] and in rigid-core complexes[7] (1.89–1.99 Å). It is, however,

Table 2 Atomic coordinates with their estimated standard deviations (e.s.d.s) in parentheses, for non-hydrogen atoms of compound **1a**

Atom	x	y	z
Fe	0.0000	0.0000	0.0000
N(1)	0.2243(4)	0.0754(5)	0.2191(4)
C(2)	0.1466(5)	−0.0027(6)	0.2447(4)
C(3)	0.1986(5)	−0.0168(6)	0.3637(5)
C(4)	0.3015(5)	0.0494(6)	0.4022(5)
C(5)	0.3174(5)	0.1068(6)	0.3116(5)
C(6)	0.3913(5)	0.1753(6)	0.2731(5)
C(7)	0.3433(5)	0.1840(6)	0.1586(5)
N(8)	0.0556(4)	−0.0423(4)	0.1689(4)
C(9)	0.1483(6)	−0.0863(7)	0.4304(6)
C(10)	0.3760(6)	0.0570(6)	0.5132(6)
C(11)	0.5001(6)	0.2254(6)	0.3402(6)
C(12)	0.3867(5)	0.2582(6)	0.0912(5)
C(13)	0.2346(5)	0.1170(5)	0.1196(5)
N(14)	0.1580(4)	0.0897(5)	0.0255(4)
N(15)	0.1105(6)	−0.1407(7)	0.4851(5)
N(16)	0.4346(5)	0.0605(6)	0.6024(5)
N(17)	0.5881(5)	0.2641(6)	0.3903(5)
N(18)	0.4240(4)	0.3240(5)	0.0421(4)
C(101)	−0.0795(9)	−0.3447(9)	0.1349(8)
O(102)	−0.1013(5)	−0.2359(6)	0.1827(5)
C(103)	−0.1759(8)	−0.247(1)	0.2440(9)
C(104)	−0.207(1)	−0.127(1)	0.273(1)
O(105)	−0.2678(7)	−0.0673(8)	0.1747(7)
C(106)	−0.302(1)	0.045(1)	0.194(1)

Table 3 Atomic coordinates with their (e.s.d.s) in parentheses, for non-hydrogen atoms of compound **2a**

Atom	x	y	z
Co	0.0000	0.0000	0.0000
N(1)	0.2189(4)	0.0764(4)	0.2162(3)
C(2)	0.1411(4)	−0.0015(5)	0.2399(4)
C(3)	0.1942(4)	−0.0167(5)	0.3602(4)
C(4)	0.2974(4)	0.0495(5)	0.4003(4)
C(5)	0.3135(5)	0.1070(5)	0.3096(4)
C(6)	0.3898(4)	0.1748(5)	0.2731(5)
C(7)	0.3402(5)	0.1820(5)	0.1565(4)
N(8)	0.0502(4)	−0.0422(4)	0.1632(3)
C(9)	0.1443(5)	−0.0876(6)	0.4262(5)
C(10)	0.3743(5)	0.0567(5)	0.5140(5)
C(11)	0.4992(5)	0.2251(5)	0.3401(5)
C(12)	0.3854(5)	0.2548(6)	0.0892(4)
C(13)	0.2304(5)	0.1151(5)	0.1175(4)
N(14)	0.1528(4)	0.0865(4)	0.0234(3)
N(15)	0.1071(5)	−0.1433(6)	0.4806(5)
N(16)	0.4342(5)	0.0590(5)	0.6028(4)
N(17)	0.5885(5)	0.2630(6)	0.3912(5)
N(18)	0.4249(4)	0.3171(5)	0.0423(4)
C(101)	−0.0800(8)	−0.3463(8)	0.1326(7)
O(102)	−0.1004(5)	−0.2391(5)	0.1816(4)
C(103)	−0.1781(7)	−0.252(1)	0.2386(7)
C(104)	−0.2067(8)	−0.133(1)	0.2720(8)
O(105)	−0.2645(6)	−0.0679(7)	0.1760(5)
C(106)	−0.298(1)	0.046(1)	0.198(1)

Table 4 Bond lengths (Å) and angled (°), with e.s.d.s in parentheses,* for compounds **1a** and **2a**

	1a (M = Fe)	**2a** (M = Co)		**1a** (M = Fe)	**2a** (M = Co)
M–N(8)	2.091(5)	2.019(5)	C(6)–C(11)	1.43(1)	1.42(1)
M–N(14)	2.090(5)	2.015(5)	C(7)–C(12)	1.415(8)	1.425(8)
M–N(18^{I})	2.295(5)	2.369(5)	C(7)–C(13)	1.45(1)	1.452(9)
N(1)–C(2)	1.398(8)	1.391(7)	C(9)–N(15)	1.132(9)	1.138(8)
N(1)–C(5)	1.38(1)	1.379(9)	C(10)–N(16)	1.13(1)	1.12(1)
N(1)–C(13)	1.400(8)	1.389(7)	C(11)–N(17)	1.13(1)	1.13(1)
C(2)–C(3)	1.45(1)	1.458(8)	C(12)–N(18)	1.150(8)	1.130(7)
C(2)–N(8)	1.281(9)	1.275(8)	C(13)–N(14)	1.29(1)	1.282(9)
C(3)–C(4)	1.39(1)	1.385(9)	C(101)–O(102)	1.41(1)	1.41(1)
C(3)–C(9)	1.430(9)	1.437(8)	O(102)–C(103)	1.39(1)	1.389(9)
C(4)–C(5)	1.392(8)	1.400(7)	C(103)–C(104)	1.46(2)	1.48(2)
C(4)–C(10)	1.41(1)	1.43(1)	C(104)–O(105)	1.39(2)	1.39(1)
C(5)–C(6)	1.386(8)	1.396(7)	O(105)–C(106)	1.36(2)	1.39(1)
C(6)–C(7)	1.39(1)	1.404(9)			
N(14)–M–N(8)	89.0(2)	91.7(2)	C(11)–C(6)–C(5)	125.4(7)	126.8(6)
N(18^{I})–M–N(8)	92.1(2)	92.1(2)	C(11)–C(6)–C(7)	125.8(5)	125.6(5)
N(18^{I})–M–N(14)	90.9(2)	92.1(2)	C(12)–C(7)–C(6)	125.0(6)	124.4(6)
C(5)–N(1)–C(2)	112.3(5)	112.6(4)	C(13)–C(7)–C(6)	109.8(5)	109.6(5)
C(13)–N(1)–C(2)	133.7(6)	133.2(5)	C(13)–C(7)–C(12)	124.8(7)	125.7(3)
C(13)–N(1)–C(5)	113.5(5)	113.4(5)	C(2)–N(8)–M	127.2(4)	125.5(3)
C(3)–C(2)–N(1)	102.9(6)	102.8(5)	N(15)–C(9)–C(3)	178.6(9)	178.4(8)
N(8)–C(2)–N(1)	120.9(6)	121.4(5)	N(16)–C(10)–C(4)	178.3(7)	178.1(7)
N(8)–C(2)–C(3)	136.2(6)	135.7(5)	N(17)–C(11)–C(6)	177.4(7)	177.4(6)
C(4)–C(3)–C(2)	109.9(5)	109.7(5)	N(18)–C(12)–C(7)	175.4(8)	175.3(7)
C(9)–C(3)–C(2)	124.2(6)	124.5(6)	C(7)–C(13)–N(1)	101.8(6)	102.6(5)
C(9)–C(3)–C(4)	125.9(7)	125.8(6)	N(14)–C(13)–N(1)	121.1(6)	120.3(5)
C(5)–C(4)–C(3)	107.8(6)	107.8(6)	N(14)–C(13)–C(7)	137.1(6)	137.0(5)
C(10)–C(4)–C(3)	126.0(6)	126.0(5)	C(13)–N(14)–M	126.7(4)	126.2(3)
C(10)–C(4)–C(5)	126.2(6)	126.1(5)	C(103)–O(102)–C(101)	115.1(8)	113.6(7)
C(4)–C(5)–N(1)	107.2(5)	107.0(5)	C(104)–C(103)–O(102)	110(1)	109.1(8)
C(6)–C(5)–N(1)	106.0(6)	106.8(5)	O(105)–C(104)–C(103)	108(1)	107.9(9)
C(6)–C(5)–C(4)	146.5(7)	145.9(7)	C(106)–O(105)–C(104)	112(1)	112.7(9)
C(7)–C(6)–C(5)	108.7(6)	107.6(6)			

* Symmetry code: I, $\frac{1}{2} - x, y - \frac{1}{2}, -z$.

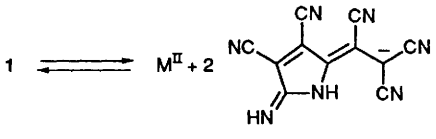

Scheme 1

comparable with values in other high-spin ($S = \frac{3}{2}$) cobalt(II) aza complexes.[8]

Solid State and Solution Properties.—In the solid state complexes **1** and **2** are stable crystalline substances, but are best protected from moisture, because of the propensity of water to replace the crystallization solvent (A). On heating (from room temperature to 300 °C) under vacuum (10^{-3} mmHg, *ca.* 0.133 Pa) they first lose A, then undergo pyrolysis releasing the free acid HL, as observed for the analogous nickel(II) complex.[1] They are moderately soluble and partially dissociated in polar solvents, affording air-sensitive, intense blue solutions; the solubility depends on the solvent (acetone > EtOH > MeCN ≫ thf ≈ dme) and on the metal (the most soluble is **1** in acetone, solubility > 10^{-2} mol dm^{-3}).

Rates and constants of dissociation in solution, which can be estimated by measuring the absorbance of the resulting pyrroline anion (λ_{max} = 546 nm, ε = 301 75 dm^3 mol^{-1} cm^{-1})[9] according to the equilibrium in Scheme 1, are both solvent and metal dependent. The stability in the common solvents under dinitrogen and under neutral conditions lies in the sequence: EtOH > acetone > MeCN ≫ dimethylformamide (dmf); the rate of equilibration is low in dmf (hours at *ca.* 10^{-3} mol dm^{-3}), and very high in other solvents. As regards the dissociation equilibrium, **1** is less stable than **2**. The observed metal complex stability order is Mn^{II} < Fe^{II} < Co^{II} < Ni^{II} > Zn^{II} which is exactly that of the σ-acceptor character of the metal(II) ions or the so-called Irving–Williams order.[10] This coincidence indicates that in our complexes only the σ-donor strength of the ligand is important and that metal-to-ligand π donation can be excluded, according to structural and spectroscopic findings.

An excess of metal(II) ion reverses the above equilibrium. On the other hand addition of water results in labilization of the ligand, particularly pronounced for the derivatives of Mn^{II}, Fe^{II} and Zn^{II}, so that the synthesis of the less-stable complexes, **1** included, requires rigorously dried solvents and anhydrous MCl_2 in order to attain quantitative yields.

Infrared Spectra.—Most interest in the IR spectra is associated with the imino >C=N–H double-bond stretching vibration, which gives a band at 1630 cm^{-1}. The intensity of this band depends markedly on the metal and on the solvent, adducted *via* hydrogen bonding, and it follows the sequence: **2a** ≈ **2b** ≈ **2c** ≫ **2d** ≈ **1a** ≈ **1d** > **1c** > **1b**. Two spectra, remarkably different in this region, due to **1b** and **2b**, are reported in Fig. 3; the band attributable to the imino group, while very strong for **2b**, is almost imperceptible for **1b**.* The very low

* The absence of the stretching frequencies in the spectrum of complex **1b** led us first to the erroneous conclusion that a saturation of the C=N double bond might have occurred; but we found, from a preliminary X-ray crystal structure determination of both **1b** and **2b**, that these complexes are isomorphous [monoclinic, space group *C*2/*c*, *a* = 12.408(3), *b* = 20.195(5), *c* = 17.035(4) Å, β = 97.88°] and isostructural, with the centrosymmetric metal atom in a tetragonally distorted octahedral co-ordination (M–N_{eq} 2.10 and 2.06 Å respectively), two thf units in apical position (M–O_{ax} of thf 2.22 and 2.18 Å respectively) and the other two laterally adducted as in the copper derivative.[3]

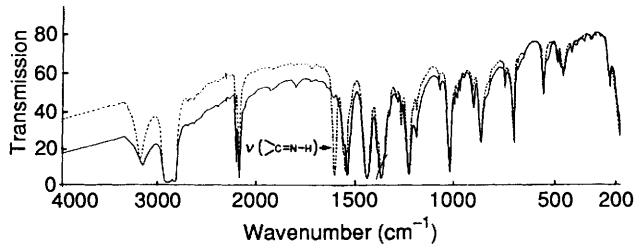

Fig. 3 Infrared spectra of complexes **1b** (——) and **2b** (– – – –) (Nujol mulls)

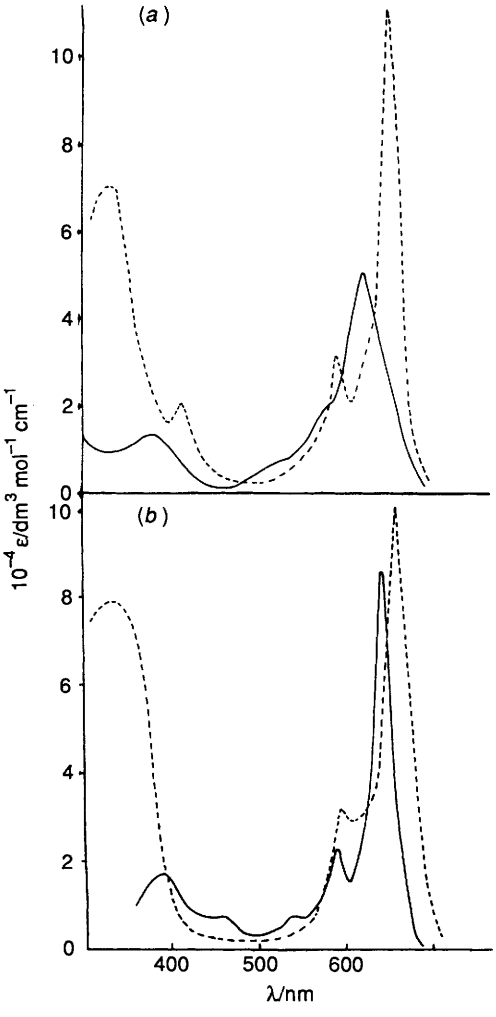

Fig. 4 Solution electronic spectra of $[ML_2]$ (——) and [M(pc)] (– – – –): (*a*) M = Fe, in MeCN + 0.1 mol dm^{-3} $[Fe(MeCN)_2Cl_2]$ and pyridine respectively; (*b*) M = Co, in acetone + 0.07 mol dm^{-3} $CoCl_2 \cdot 6H_2O$ and pyridine respectively

intensity of this band for all four iron(II) complexes is unusual. However, it compares with that observed for the cobalt(II) complex **2d** and with results reported for another iron(II) imino complex, $[Fe(NH{=}CHCOCOCH{=}NH)_3]I_2$,[11] which shows no IR absorptions above 1450 cm^{-1}.

Another prominent feature of the IR spectra concerns the highest-energy band, centred at 3300–3200 cm^{-1}, due to the N–H stretching vibrations, and appearing either broadened (**1b** and **2b**) or split into two well resolved peaks (**1c** and **2c**) and red-shifted with respect to the free ligand, not hydrogen bonded, as in the tetraphenylarsonium salt {$[AsPh_4][L]$: ν(N–H) 3360 cm^{-1}, sharp peak}.[9] This band is diagnostic of the particular hydrogen bond in **1** and **2**, formed between the two coplanar pyrrolizinido moieties and the crystallization solvent. Following the Novak classification,[12] it is a weak hydrogen bond (relative energy shift with respect to the free ligand, not engaged in hydrogen bond, < 12%). This hydrogen bond causes an interligand vibrational coupling of the two coplanar N–H groups, which can explain the observed splitting of the corresponding IR bands. Instead, intraligand coupling cannot account for the observed splitting, as shown by normal coordinate analysis by Armendarez and Nakamoto[13] and experimental data on similar metal complexes, for instance on the metal bis(oxamides) $[M^{II}\{HNC(O)C(O)NH\}_2]^{2-}$ (M = Ni, Cu or Pd) [ν(N–H) 3310 cm^{-1}, sharp single band].

Electronic Spectra.—As observed for the analogous nickel(II) complex,[1] the solution visible electronic spectra of **1** and **2** are solvent independent and very similar to those of the corresponding phthalocyaninates (Fig. 4). Complex **1** shows a spectrum less intense than that of **2** because it is more dissociated in solution, according to the metal and solvent stability orders given above. Although the two systems, phthalocyaninates and pyrrolizinides, are very different, the two spectra are surprisingly similar: (*i*) the lowest-energy intense band (Q band) exhibits higher-energy vibrational components; (*ii*) there is a characteristic window in the 500 nm region; (*iii*) the highest-energy (Soret) band displays a shoulder to low energy.

Molecular orbital calculations with the semiempirical INDO/S method are in progress[14] on the two systems in order to cast light on these spectroscopic similarities. At present only a tentative empirical assignment of the electronic spectra of the pyrrolizinides, based on the analogy with phthalocyaninates and taking into account the different symmetries (D_{2h}, D_{4h}), is possible (see Table 5). In both systems the two bands have the same origin [π_u (highest occupied molecular orbital, HOMO) ⟶ π_g^* (lowest occupied molecular orbital, LUMO)] and in our system there are two LUMO orbitals (b_{2g} and b_{3g}, correlated with e_g in D_{4h}), nearly degenerate, although not required by symmetry. Therefore the planar $[ML_2]$ system seems to behave as a tetrapyrrolic macrocycle as regards the ligand π orbitals. Thus, extensive conjugation between the two pyrrolizinido moieties, brought into close proximity and in plane *via* co-ordination, should occur through the metal ion; the degree of such 'interligand through metal conjugation' depends on the M–N bond distance. Indeed, complex **1** is less conjugated than **2** (longer M–N bonds) and consequently both the Q and Soret bands of **1** are shifted to shorter wavelength with respect to **2**. Even [Fe(pc)] (pc = phthalocyaninate) displays a slightly blue-shifted Q band compared to [Co(pc)], explained in the literature as due to the stronger π back bonding M⟶L in [Fe(pc)] which lifts the ligand e_g^* orbital.[15] This effect can be excluded in our case, because the long Fe–N bond minimizes the metal to ligand back donation, if any.

Finally the diffuse reflectance spectra show extra low-energy bands (1030, **1a**; 1160 and 850 nm, **2a**), absent in solution, which may well be spin-allowed d–d transitions, confined to the tetragonally distorted $MN_4N'_2$ chromophore and typical of six-co-ordinated high-spin complexes of Fe^{II} and Co^{II}.

Magnetic Measurements.—The magnetic susceptibility data are shown in Fig. 5. Complex **1a**, by showing at high temperature (170–300 K) a Curie–Weiss linear behaviour with μ_{eff} = 4.28 corresponding to four, weakly antiferromagnetically coupled, unpaired electrons, is a high-spin (S = 2) species. No EPR signal was obtained from it. Complex **2a** exhibits a more complicated variable-temperature magnetic susceptibility: its magnetic moment gradually increases from 1.97 (6–60 K) to 3.65 (265–300 K), probably a result of a strong intermolecular 180° superexchange coupling between the magnetic electrons of adjacent high-spin ($S = \frac{3}{2}$) cobalt(II) ions (broad structureless EPR signal, g = 2.221). More specifically, the main interaction,

Table 5 Absorption maxima (nm) (ε/dm³ mol⁻¹ cm⁻¹ in parentheses) of the main electronic bands and their assignments (experimental conditions as in Fig. 4)

Compound				Assignment *	
[Fe(pc)]	[Co(pc)]	**1**	**2**	D_{2h}	D_{4h}
		623 (53 000)	645 (86 000)	$a_u(\pi) \longrightarrow b_{2g}, b_{3g}(\pi^*)$	
		380 (13 200)	393 (17 500)	$b_{1u}(\pi) \longrightarrow b_{2g}, b_{3g}(\pi^*)$	
654 (113 000)	658 (101 000)				$a_{1u}(\pi) \longrightarrow e_g(\pi^*)$
332 (71 100)	330 (79 200)				$a_{2u}(\pi) \longrightarrow e_g(\pi^*)$

* The assignment for [M(pc)] is from ref. 15.

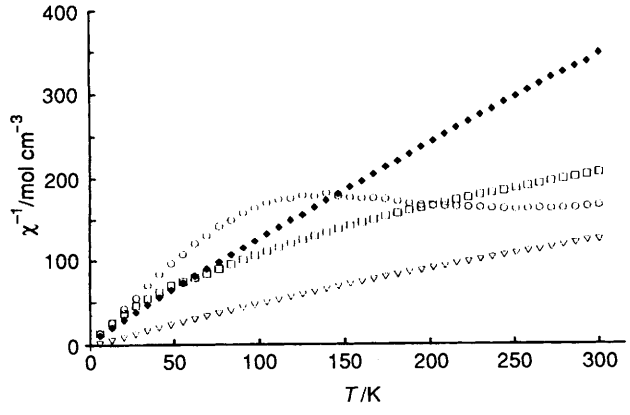

Fig. 5 Temperature dependence of the reciprocal molar susceptibility for the compounds **1a** (▽), **2a** (○), **3** (◆) and **4** (□)

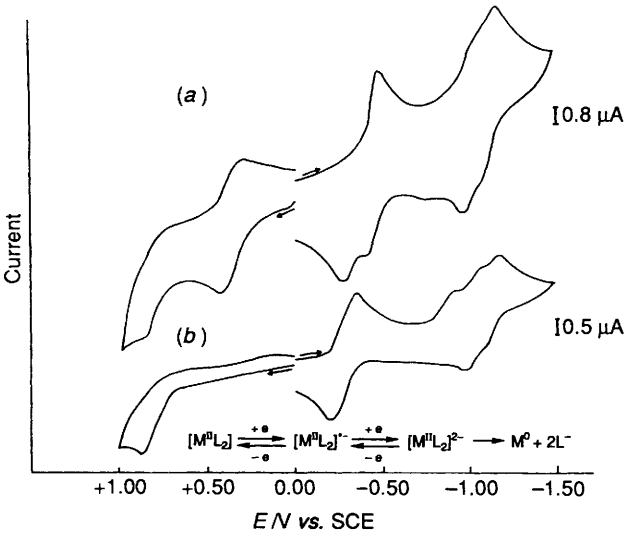

Fig. 6 Cyclic voltammetry of $[FeL_2]$ (*a*) and $[CoL_2]$ (*b*) (1 mmol dm^{-3}) at a platinum electrode in dmf with 0.1 mol dm^{-3} NEt_4ClO_4 (scan rate 200 mV s^{-1})

which gives antiparallel coupling, is of σ type between two magnetic cobalt orbitals pointing toward each other, mediated by a filled, overlapping, intervening ligand orbital of appropriate symmetry. The dominant exchange pathway for this interaction in **2a** is thus $d'_{z^2}\|\sigma_L(b_{1g})\|d_{x^2-y^2}$ where d'_{z^2} refers to the orbital of one metal atom, $d_{x^2-y^2}$ to that of the next nearest-neighbouring metal atom, and ‖ symbolizes overlap. The antiferromagnetic coupling in **1a** is much weaker than in **2a** for several reasons: in **1a** the M–N bond distance is longer, thus lowering the $\sigma_L(b_1)_g\|d_{x^2-y^2}$ term and the number of magnetic electrons (n) is higher, again a factor operating in the same direction, given that the magnitude of the coupling depends on $1/n^2$.[16]

Returning to the analogy with tetrapyrrolic macrocycles, it is pertinent to make a comparison with the magnetic data of the corresponding phthalocyaninate species containing a similar $MN_4N'_2$ chromophore, *i.e.* [Fe(pc)]·2py[17] and [Co(pc)]·2py (py = pyridine),[18] both low-spin complexes. We conclude that the ligand-field strength of the tetracyanopyrrolizinide is lower than that of phthalocyanine, and is influenced by the presence of the electron-withdrawing CN groups and by the fact that the negative charge is not localized on the nitrogen atoms directly bound to the metal.

Electrochemical Behaviour.—In Fig. 6 the cyclic voltammetry (CV) results of forward and reverse scans of both reduction and oxidation are presented. Reduction waves indicate the presence of many quasi-reversible processes, as observed for the nickel(II) analogue.[1] Exhaustive coulometric reductions at controlled potential 0.1 V more negative than the first cathodic peak potential [E_{pc} −0.48 **1**; and −0.35 V *vs.* saturated calomel electrode (SCE) **2**] were performed in several solvents, containing different supporting electrolytes. In each case a two-electron transfer was observed and the solution became violet upon formation of an equivalent amount of the free ligand, which is stable under the working conditions (E_{pc} −0.94 V *vs.* SCE);[9] the overall two-electron reduction may be described as in Fig. 6. The radical monoanion $[ML_2]^{\bullet-}$, initially formed upon addition of the first electron, cannot be trapped in an insoluble salt after combination with a suitable cation before being reduced further to dianion as in the case of the nickel(II) complex, whereupon the dianion disproportionates leading to demetallation, on the electrochemical time-scale.

Note that complex **2** is reduced more easily than **1**. Assuming that the ligand is the part preferentially reduced as in the nickel(II) complex [on the other hand, the shape of the reduction waves for **1**, **2** and the nickel(II) complex is very similar], this fact may be explained by again invoking the higher conjugation of the ligand system in **2** than in **1** (the M–N bond distance is shorter in **2**), *i.e.* an increase in electron delocalization in **2** leads to its easier reduction. A correlation can then be established between the energy of the electronic bands and the magnitude of the reduction potential in our system, in the sense that they both depend on the degree of 'interligand through metal conjugation', as revealed by the M–N bond distances.

Finally complex **1** can be oxidized as well as reduced, at relatively low anodic potential (E_p for **1** +0.44 V *vs.* SCE). This oxidation process certainly involves the metal because it has no counterpart in the voltammograms of any other $[ML_2]$ complex, and it is not reversible on the electrochemical time-scale. Attempts to obtain the oxidation product electrochemically were unsuccessful, and at the end of the electrolysis the solution became violet upon formation of the ligand. These observations are consistent with the fact that iron(III) ion does not give complexes with L, but is instead reduced to Fe^{II} (see Experimental section).

Interaction with O_2.—*Synthesis and hypothetical structure of the oxidation products.* Complexes **1** and **2** react slowly and irreversibly with dioxygen in solution, to produce compounds corresponding stoichiometrically to the formulae $[FeL_3(O_2)]$·

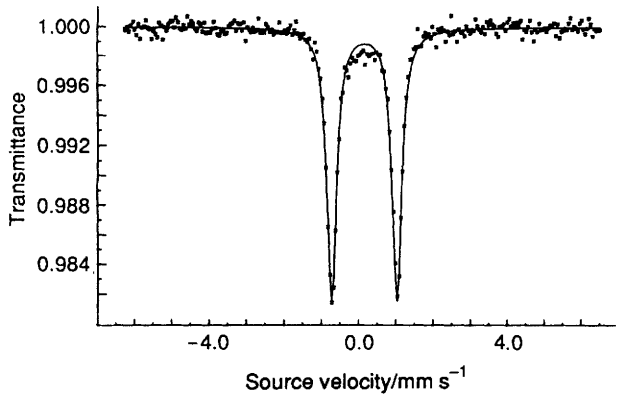

Fig. 7 Mössbauer spectrum of compound **3**. The weak signals within the doublet arise from high-spin iron(III) impurities

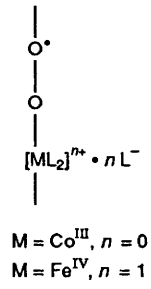

6MeCN **3** and $[CoL_2(O_2)]$·4MeCN **4**. Unfortunately attempts to grow single crystals, suitable for X-ray diffraction studies, were unsuccessful, owing to their very low solubility. Nevertheless an axially polymerized chain structure, containing a monomer with bridging superoxide $O_2^{\bullet -}$ and the metal in the oxidation states IV and III respectively, could be inferred from different chemicophysical measurements: (*i*) the presence in **3** of a free, charge-compensating, unco-ordinated counter ion L is confirmed by the absorption at 550 nm in the reflectance spectrum; (*ii*) the IR spectra of **3** and **4** are very similar to those of **1c** and **2c** respectively; (*iii*) in addition, they both are insensitive to $^{16}O_2$ by $^{18}O_2$ substitution, a fact indicating that the M–O–O–M bridge is centrosymmetric;[19] (*iv*) the mass spectra of $^{18}O_2$ derivatives from room temperature to 300 °C reveal loss of only solvated acetonitrile, a fact indicating that O_2 is negatively charged and consistent with the irreversibility of O_2 uptake.

The magnetic data (Fig. 5) support the formula given, from which not only the metal is expected to contribute to the magnetic moment, but also the μ-superoxide $O_2^{\bullet -}$ radical. The behaviour of both **3** and **4** approaches the Curie–Weiss expression at high temperature, with μ_{eff} of 2.59 and 3.20 respectively.

In the case of **3** the sample is contaminated with a small amount of high-spin iron(III) impurities as revealed by the Mössbauer spectrum (Fig. 7), and therefore its magnetic moment can be interpreted as due to only one unpaired electron per iron atom, consistently also with its EPR spectrum, attributable to one unpaired electron, of axial magnetic symmetry with two principal g values ($g_1 = 2.103, g_2 = 1.959$). Mössbauer data (isomer shift = 0.168 mm s^{-1}, quadrupole splitting = 1.754 mm s^{-1}) are consistent with either low-spin Fe^{III} ($S = \frac{1}{2}$) or Fe^{IV} ($S = 1$) tetraaza macrocycles,[20] in a tetragonally elongated iron site symmetry. All these observations could be rationalized in a molecular orbital scheme in which the $O_2^{\bullet -}$ unpaired electron is strongly antiferromagnetically coupled with an unpaired iron(IV) d^4 ($S = 1$) electron, giving rise on the whole to a one-electron paramagnetic iron(IV) compound.

Although, at present, we have no direct experimental information allowing the assignment of **3** as a iron(IV) compound, this hypothesis remains the most reasonable among others possible, which involve low-spin iron(III) species, and yet consistent with both magnetic and Mössbauer data, such as Fe^{III} $(O_2^{\bullet -})$-$(L^-)_2L^{\bullet}$ or $Fe^{III}(L^-)_2(LO_2)^-$: no spectroscopic evidence exists for them; moreover, the implied ligand-based oxidation or oxygenation is unlikely, given the poor electron-donating ability of the pyrrolizinido moiety (L^-).

No simple explanation can be found for the magnetic data for complex **4**. Its magnetic behaviour, in fact, is consistent with a three-unpaired-electron species as if the $O_2^{\bullet -}$ electron barely interacts with the two unpaired cobalt(III) d^6 electrons; however it is EPR silent (in contrast with the occurrence of the strong EPR signal of the precursor **2a**), and therefore not easily accountable, unless very short relaxation times are invoked in **4**.

Also electron spectroscopy for chemical analysis (ESCA) data (Table 6) provide further support for the formula given: negative binding energy shifts for the 1s oxygen peak are observed in **3** and **4** relative to the OMe oxygen of dme in the precursors **1a** and **2a**. This negative shift, from 1.6 to 1.9 eV, is in agreement with that found (1.1–1.9 eV) for oxidized cobalt(II) Schiff-base complexes.[21] Furthermore, the M/O atomic ratio, obtained by comparing the area of metal $2p_{\frac{3}{2}}$ and oxygen 1s peaks, in accord with the procedure proposed by Wagner *et al.*,[22] is close to the expected value of 0.5:1. The binding energies of the core electrons of the metals are also informative: in **3** and **4** they are larger by 0.6–0.7 eV than in the precursors **1a** and **2a**.

Unfortunately resonance-Raman spectra, recorded as described below (see Experimental section), of the $^{16}O_2$ and $^{18}O_2$ derivatives, of both **3** and **4**, were laser identical (probably because of photochemical decomposition by the laser beam), and thus of no diagnostic value in assessing the amount of negative charge localized on the bridging dioxygen.

Finally it is noteworthy to compare the reactivity towards oxygen of the complexes and the analogous phthalocyaninates: [Fe(pc)] and [Co(pc)] have been found to react with oxygen to form 2:0.5 and 1:1 M:O_2 compounds respectively, and in particular a μ-oxo iron(III) dimer[23] and a dioxygen adduct of Co^{II}, stable only at low temperature.[24] Complexes **1** and **2** are therefore more easily metal-oxidized than are phthalocyaninates, consistent with a higher negative charge on the metal as expected from the poor π-acceptor pyrrolizinido ligand.

Properties of Complexes **3** *and* **4**.—These complexes are insoluble (even in dmf), moisture sensitive and electrical insulators. The most interesting property is the electronic spectrum; the Q band (λ_{max}: 680 **3**, 712 nm **4**) is red-shifted by about 60–70 nm compared to the precursors **1** and **2** (see Table 5). This shift has been detected in MeCN solutions of **1** and **2**, when exposed to oxygen, and is confirmed by the reflectance spectra of **3** and **4**. No isosbestic points are observed during the oxygenation of **1** and **2** in solution, since the scarcely soluble **3** and **4** partially separated as soon as they were formed. This red shift of the Q band may again be explained as due to an increase in the 'interligand through metal conjugation' in **3** and **4** with respect to **1** and **2**. The M–N bond distances in **3** and **4** are probably shorter than in **1** and **2** respectively, because the metal-ion size is decreased following oxidation.

Experimental

General.—Details of some chemicophysical measurements (elemental analysis, IR, UV and ESCA spectra, cyclic voltammetry, coulometry) have been given earlier.[1] Magnetic measurements were carried out on a commercial SQUID magnetometer (Quantum Design, H_{max} = 5 T); molar susceptibilities were corrected for intrinsic diamagnetism, estimated from Pascal's constants including constitutive corrections. The mass spectra were measured with a V.G. micromass 7070 F instrument

Table 6 Nitrile carbon, nitrogen, oxygen and metal binding energies (eV) * from X-ray photoelectron spectra and M/O atomic ratios (in parentheses)

		N 1s				O 1s	
Sample	C 1s (–C≡N)	–C≡N	N	=NH	M $2p_{\frac{3}{2}}$	Superoxo	OMe
1a	283.4	397.5	398.7	399.9	709.2		530.9
2a	283.5	397.4	398.9	400.0	780.3		530.9
3	283.4	397.7	398.6	399.8	709.9	529.0 (0.59)	
4	283.4	397.6	398.8	399.8	780.9	529.3 (0.45)	

* Referenced to the C 1s pump-line oil hydrocarbon peak (285.0 eV).

(electron impact, 70 eV; emission current, 200 μA), located at Servizio GC-MS of Area della Ricerca di Roma.

The resonance-Raman spectra were measured on pressed, not spinning, neat powder pellets, at room temperature in a quasi-back scattering mode; a Triple spectrometer, Spex model 1877, equipped with a 600 lines per mm grating, an OMA CCD EG&G Princeton detector and an argon-ion laser as the excitation source, providing 5145, 4880, 4765 and 4579 Å lines, was used; the incident laser power was 10 mW.

Mössbauer spectra were recorded at liquid-nitrogen temperature on a conventional constant-acceleration spectrometer, which utilizes a room-temperature rhodium matrix cobalt-57 source. The EPR spectra were recorded on undiluted polycrystalline samples with an X-band Varian spectrometer.

Materials.—Solvents were carefully dried, freshly distilled and degassed before use. The $^{18}O_2$ gas (97% enriched) was purchased from Merck Frost, Canada. Anhydrous iron chlorides were prepared according to known procedures, starting from commercial $FeCl_3 \cdot 6H_2O$ *via* $FeCl_3$[25] to $[Fe(MeCN)_2Cl_2]$.[26] Commercial [Fe(pc)] and [Co(pc)] were purified by sublimation. The ligand L was prepared, as its sodium salt, from tetracyanoethylene according to our procedure.[27] The preparation of complex **1b** was given previously,[3] starting from the ligand as its tetraphenylarsonium salt and $FeCl_2$ in anhydrous thf; later we realized that $FeCl_2$, when rigorously dried, is completely insoluble in anhydrous thf and the reaction with L does not occur; so in the earlier syntheses some adventitious water was involved in the reaction, causing irreproducible results. We give here a reproducible preparation of the complex **1a** starting from $[Fe(MeCN)_2Cl_2]$ in MeCN, a solvent in which the iron salt is quite soluble ($\approx$0.3 mol dm^{-3}).

Syntheses.—$[FeL_2]$·2dme **1a**. The salt NaL (0.50 g, 1.96 mmol) was added to a MeCN solution (100 cm^3) of $[Fe(MeCN)_2Cl_2]$ (1.5 g, 7.69 mmol) at room temperature under N_2. The resulting intense blue solution was stirred for 2 h at room temperature. Evaporation to dryness left a brown residue, which was washed with water and then with thf. After refluxing with dme for 10 min and filtering, complex **1a** was obtained as golden microcrystals (0.55 g, 80%) (Found: C, 51.30; H, 3.40; Fe, 7.90; N, 27.95; O, 9.05. $C_{30}H_{24}FeN_{14}O_4$ requires C, 51.45; H, 3.45; Fe, 7.95; N, 28.00; O, 9.15%). The same product, but less pure and in lower yield, was obtained by using $FeCl_3$ in dme. Suitable crystals for X-ray diffraction studies were grown in a sealed vial from a saturated solution of dme–MeCN (3:7), by slow cooling from 80 °C to room temperature over 7 d.

Complexes **1b**–**1d** were easily obtained by refluxing **1a** for a few minutes in the corresponding anhydrous solvent under N_2.

$[CoL_2]$·2dme **2a**. The salt NaL (0.5 g, 1.96 mmol) was added to acetone–water (7:3, 90 cm^3) containing $CoCl_2 \cdot 6H_2O$ (3.0 g, 12.6 mmol) under N_2. The resulting blue solution was quickly evaporated under vacuum to 30 cm^3. After filtration, washing with water and drying, the residue was refluxed with anhydrous dme; complex **2a** (0.63 g, 92%) was collected as bronze microcrystals (Found: C, 51.40; H, 3.35; Co, 8.20; N, 27.75; O, 9.00. $C_{30}H_{24}CoN_{14}O_4$ requires C, 51.20; H, 3.45; Co, 8.40; N, 27.85; O, 9.10%). Large single crystals of **2a** and the derivatives **2b**–**2d** were obtained as for the analogous iron(II) complexes.

$[FeL_3(O_2)]$·6MeCN **3**. Complex **1a** (0.3 g, 0.42 mmol) was added to MeCN (30 cm^3) under N_2. The blue suspension was exposed to dry oxygen (dried over KOH) for 4 d with stirring at room temperature. Its colour changed slowly to violet and a microcrystalline black solid separated. The reaction vessel was again filled with N_2 and transferred to a dry-box, where the solid was filtered off, washed with MeCN, dried and collected (0.18 g) (Found: C, 52.05; H, 1.85; Fe, 5.25; N, 37.75; O, 3.10. $C_{45}H_{24}FeN_{27}O_2$ requires C, 52.45; H, 2.35; Fe, 5.40; N, 36.70; O, 3.10%). From the IR spectrum it is water-free and contains the unco-ordinated free ligand [ν(C=N–H) 1625vs cm^{-1}].

$[CoL_2(O_2)]$·4MeCN **4**. Starting from complex **2a** and operating in the same manner as for **3**, complex **4** was obtained as a blue, water-free, microcrystalline solid (0.26 g, 85%) (Found: C, 50.25; H, 2.00; Co, 8.10; N, 35.25; O, 4.45. $C_{30}H_{16}CoN_{18}O_2$ requires C, 50.10; H, 2.25; Co, 8.20; N, 35.05; O, 4.45%).

The ^{18}O-labelled derivatives of **3** and **4** were prepared simultaneously in just one run by connecting the reaction vessels containing **1a** and **2a** in MeCN to the same flask containing $^{18}O_2$ gas.

X-Ray Crystallography.—Data collection. Some difficulties were experienced in selecting satisfactory crystals of compounds **1a** and **2a**. Since they are moisture sensitive a single crystal of each was sealed in a glass capillary, in the presence of mother-liquor. Preliminary examination by oscillation and Weissenberg photographs showed that they are isomorphous, with monoclinic symmetry. The space group $P2_1/a$ was chosen on the basis of the axial lengths and systematic absences. Lattice constants (Table 1) were obtained from a least-squares refinement that utilized the setting angles of 25 automatically centred reflections. X-Ray intensity data were measured by θ–2θ scan employing graphite-monochromated Mo-Kα radiation (λ 0.710 69 Å) on a computer-controlled Nicolet $P2_1$ four-circle diffractometer. Two standard reflections, measured every 50 during data collection, showed no trend with exposure to the X-ray beam. Although the linear absorption coefficients (Table 1) are not large, a semiempirical absorption correction, based on a ψ scan around the scattering vector of selected reflections, was applied. Data for which $I > 3\sigma(I)$ were taken to be observed, leading to 1683 unique reflections for **1a** and 1852 for **2a**.

Solution and refinement of the structures. The structure of complex **1a** was solved by conventional Patterson and Fourier methods. The same non-hydrogen atomic coordinates were used as initial coordinates for compound **2a**. Both structures were then refined by full-matrix least-squares methods, using anisotropic thermal parameters for all non-hydrogen atoms; hydrogens were placed in their idealized positions and restrained to ride on their associated atoms. The quantity minimized was $\Sigma w(|F_o| - |F_c|)^2$, where $w = 1/[\sigma(F_o)]^2$. The final R $(= \Sigma||F_o| - |F_c||/\Sigma|F_o|)$ and R' $\{= [\Sigma w(|F_o| - |F_c|)^2/\Sigma w(F_o)^2]^{\frac{1}{2}}\}$ were 0.065 and 0.063 respectively for compound **1a**, and 0.062 and 0.063 for **2a**. Neutral scattering factors, f' and f'' values were taken from ref. 28. Final atomic coordinates for non-hydrogen atoms are listed in Tables 2 and 3.

Calculations were carried out on a Data General Eclipse/8000 II computer, by using the SIR CAOS crystallographic program system.[29]

Additional material available from the Cambridge Crystallographic Data Centre comprises H-atom coordinates and thermal parameters.

Acknowledgements

We thank Dr. G. Righini for the ESCA measurements, Dr. D. Attanasio for EPR spectra, Professor U. Russo of Padova University for the Mössbauer spectra, Dr. G. Mattei for the resonance-Raman spectra, Mr. E. Brancaleoni for the mass spectra, Mr. C. Veroli for drawings and technical assistance and the Progetto Finalizzato Materiali Speciali del C.N.R. for financial support.

References

1 M. Bonamico, V. Fares, A. Flamini and N. Poli, *Inorg. Chem.*, 1991, **30**, 3081.
2 A. L. Thomas, *Phthalocyanines Research and Applications*, CRC Press, Baton Rouge, FL, 1990.
3 M. Bonamico, V. Fares, A. Flamini, P. Imperatori and N. Poli, *Angew. Chem., Int. Ed. Engl.*, 1989, **28**, 1049.
4 (*a*) C. T. Chen, D. S. Liaw, G. H. Lee and S. M. Peng, *Transition Met. Chem. (Weinheim)*, 1989, **14**, 76; (*b*) S. M. Peng, C. T. Chen, D. S. Liaw, C. I. Chen and Y. Wang, *Inorg. Chim. Acta*, 1985, **101**, L31; (*c*) M. Tahiri, P. Doppelt, J. Fisher and R. Weiss, *Inorg. Chem.*, 1988, **27**, 2897; (*d*) F. Cariati, F. Morazzoni and M. Zocchi, *J. Chem. Soc., Dalton Trans.*, 1978, 1018; (*e*) K. Bowman-Mertes, P. W. R. Corfield and D. H. Busch, *Inorg. Chem.*, 1977, **16**, 3226; (*f*) L. J. Radonovich, A. Bloom and J. L. Hoard, *J. Am. Chem. Soc.*, 1972, **94**, 2073.
5 J. F. Kirner, W. Dow and W. R. Scheidt, *Inorg. Chem.*, 1976, **15**, 1685; J. P. Collman, J. L. Hoard, N. Kim, G. Lang and C. A. Reed, *J. Am. Chem. Soc.*, 1975, **97**, 2676.
6 O. P. Anderson, A. B. Kopelove and D. K. Lavallee, *Inorg. Chem.*, 1980, **19**, 2101; J. B. Jameson, F. S. Molinaro, J. A. Ibers, J. P. Collman, J. I. Braumann, E. Rose and K. S. Suslick, *J. Am. Chem. Soc.*, 1978, **100**, 6769.
7 J. C. Stevens, P. J. Jackson, W. P. Schammel, G. G. Cristoph and D. H. Busch, *J. Am. Chem. Soc.*, 1980, **102**, 3283; B. N. Figgis, E. S. Kucharski and P. A. Reynolds, *J. Am. Chem. Soc.*, 1989, **111**, 1683; F. Cariati, F. Morazzoni and M. Zocchi, *Inorg. Chim. Acta*, 1975, **14**, L31; K. M. Kadish, C. Araullo-McAdams, B. C. Han and M. M. Frauzen, *J. Am. Chem. Soc.*, 1990, **112**, 8364; R. Mason, G. A. Williams and P. E. Fielding, *J. Chem. Soc., Dalton Trans.*, 1979, 676; R. G. Little and J. A. Ibers, *J. Am. Chem. Soc.*, 1974, **96**, 4440.
8 J. W. Egan, B. S. Haggerty, A. L. Rheingold, S. C. Sendlinger and K. H. Theopold, *J. Am. Chem. Soc.*, 1990, **112**, 2445; L. G. Armstrong, L. F. Lindoy, M. McPartlin, G. M. Mockler and P. A. Tasker, *Inorg. Chem.*, 1977, **16**, 1665.
9 M. Bonamico, V. Fares, A. Flamini, A. M. Giuliani and P. Imperatori, *J. Chem. Soc., Perkin Trans. 2*, 1988, 1447.
10 S. F. A. Kettle, *Coordination Compounds*, Nelson, Bath, 1969, p. 48.
11 D. H. Busch and J. C. Bailar, jun., *J. Am. Chem. Soc.*, 1956, **78**, 1137.
12 A. Novak, *Struct. Bonding (Berlin)*, 1974, **18**, 177.
13 P. X. Armendarez and K. Nakamoto, *Inorg. Chem.*, 1966, **5**, 796.
14 S. Nakamura, V. Fares and A. Flamini, unpublished work.
15 P. S. Braterman, R. C. Davies and R. J. P. Williams, *Adv. Chem. Phys.*, 1964, **7**, 359.
16 T. R. Waite, *J. Chem. Phys.*, 1960, **33**, 256.
17 A. B. P. Lever, *J. Chem. Soc.*, 1965, 1821.
18 F. Cariati, D. Galizioli, F. Morazzoni and C. Busetto, *J. Chem. Soc., Dalton Trans.*, 1975, 556.
19 K. Nakamoto, *Coord. Chem. Rev.*, 1990, **100**, 363.
20 W. Hiller, J. Strähle, A. Datz, M. Hanack, W. E. Hatfield, L. W. ter Haar and P. Gütlich, *J. Am. Chem. Soc.*, 1984, **106**, 329.
21 J. H. Burness, J. C. Dillard and L. T. Taylor, *J. Am. Chem. Soc.*, 1975, **97**, 6080.
22 C. D. Wagner, L. E. Davis, M. V. Zeller, J. A. Taylor, R. M. Raymond and L. M. Gale, *Surf. Interface Anal.*, 1981, **3**, 211.
23 C. Ercolani, M. Gardini, K. S. Murray, G. Pennesi and G. Rossi, *Inorg. Chem.*, 1986, **25**, 3972.
24 F. Cariati, D. Galizioli, F. Morazzone and C. Busetto, *J. Chem. Soc., Dalton Trans.*, 1975, 556.
25 A. R. Pray, *Inorg. Synth.*, 1957, **5**, 153.
26 B. J. Hathaway and D. G. Holah, *J. Chem. Soc.*, 1964, 2408.
27 A. Flamini and N. Poli, *Ital. Pat.*, 22 867-A/89, 1989.
28 *International Tables for X-Ray Crystallography*, Kynoch Press, Birmingham, 1974, vol. 4.
29 M. Camalli, D. Capitani, G. Cascarano, S. Cerrini, C. Giacovazzo and R. Spagna, *Ital. Pat.*, 3543c/86, 1986.

Received 6th July 1992; *Paper* 2/03590A